

PLASMA CHARACTERISTICS OF QUASI-STEADY MPD ARCJETS FOR MATERIAL PROCESSING

**Hirokazu Tahara, Tetsuji Shibata, Kazunori Mitsuo, Atsushi Shirasaki,
Yoichi Kagaya and Takao Yoshikawa**

Graduate School of Engineering Science, Osaka University
1-3, Machikaneyama, Toyonaka, Osaka 560-8531, JAPAN

Phone: +81-6-6850-6178

Fax: +81-6-6850-6179

E-mail: tahara@me.es.osaka-u.ac.jp

Abstract

In magneto-plasma-dynamic (MPD) arcjet generators, plasma is accelerated by electromagnetic body forces. The MPD arcjet generator can produce higher-velocity, higher-temperature, higher-density and larger-area plasmas than those of conventional thermal plasma torches. Two types of MPD arcjet generators were developed for applications of them to ceramic spray coatings. One was provided with a cathode covered with Mullite or Zirconia ceramics and the other with a titanium cathode. The former was operated with Ar for Mullite or Zirconia coating due to ablation process of the cathode cover and the latter with N₂ for titanium nitride coating due to reactive process between ablated titanium particles and nitrogen plasma. The MPD spray process could successfully form dense, uniform and hard ceramic coatings. In titanium nitride reactive spraying, plasma diagnostic measurement and flowfield analysis were also carried out. A large amount of N and N⁺ was expected to be exhausted with a high velocity from the MPD generator. Both the electron temperature and the electron number density were kept high at a substrate position compared with those for conventional low-pressure thermal sprayings. A chemically active plasma with excited particles of N⁺, Ti, Ti⁺ and Ti²⁺ were expected to contribute to better titanium nitride coatings. All coating characteristics showed that the MPD arcjet generators had high potentials for ceramic spray coatings.

1. Introduction

The quasi-steady magneto-plasma-dynamic (MPD) arcjet generator is a promising plasma accelerator, which has a coaxial electrode structure similar to those of conventional plasma torches¹⁾. However, their acceleration mechanisms are different; that is, the MPD arcjet generator, as shown in Fig.1, utilizes principally electromagnetic acceleration of the interaction between the discharge current of kiloamperes and the magnetic field azimuthally induced by the discharge current, although the working gas is accelerated aerodynamically through a straight or convergent-divergent nozzle in a thermal arcjet generator. The entire electromagnetic force is theoretically proportional to the square of discharge current. Also, the MPD discharge feature, the acceleration process and the exhaust plume feature can be widely controlled by applications of external magnetic fields²⁻⁴⁾. Accordingly, MPD arcjet generators can produce higher-velocity, higher-temperature, higher-density and larger-area plasmas than those of conventional plasma sources in MW-class input power repetitive pulsed operations. The discharge plasmas are expected to be utilized for various material manufacturing processes⁵⁻⁹⁾.

In the present study, two types of MPD arcjet generators are developed for applications of them to ceramic spray coatings. One is provided with a cathode covered with Mullite or Zirconia ceramics and the other with a titanium cathode. The former is operated with Ar for Mullite or Zirconia spray coating due to ablation of the cathode cover and the latter with N₂ for titanium nitride spray coating due to reactive process between ablated titanium particles and nitrogen plasma. Operational characteristics of the MPD arcjet generators are examined. Discharge voltages and ablation rates of ceramic materials or a titanium cathode are measured, and front velocities of ablated atoms of ceramic component are also estimated using a streak camera. Their cross sections are observed with a scanning electron microscope (SEM), and their surfaces are analyzed by means of x-ray diffraction (XRD) and x-ray photoelectron spectroscopy (XPS). The Vickers hardness is also measured. In titanium nitride reactive spray coating, plasma diagnostic measurement and flowfield analysis are carried out to understand plasma features and plasma acceleration processes and to

clarify relationships between the coating characteristics and the plasma flow characteristics.

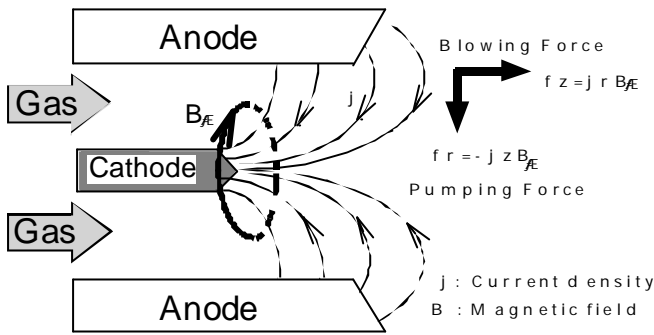


Fig.1 Electromagnetic plasma acceleration principle in a magneto-plasma-dynamic (MPD) arcjet generator.

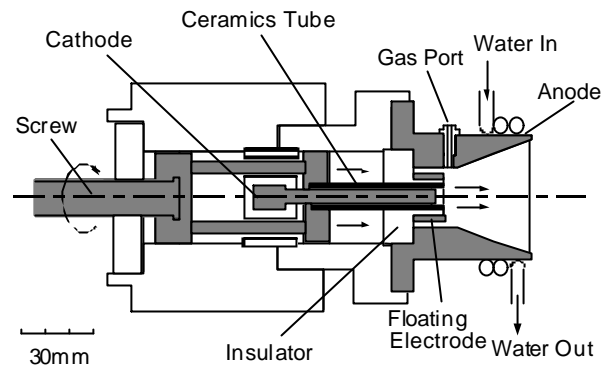


Fig.2 Cross sectional view of the MPD arcjet with the ceramic cover for Mullite and Zirconia spray coatings.

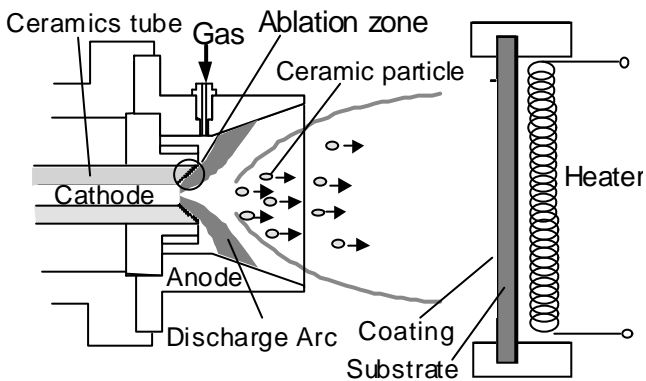


Fig.3 Illustration of ceramic spraying using the MPD arcjet generator with the ceramic cover coating.

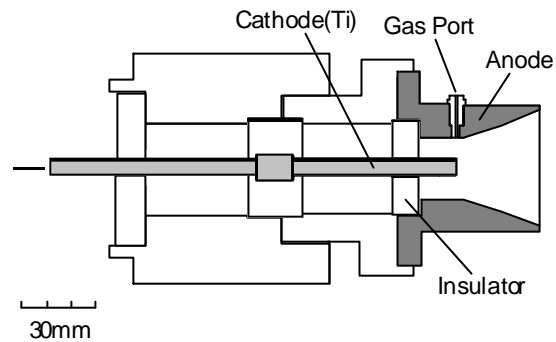


Fig.4 Cross section view of the cathode-ablation-type MPD arcjet generator for titanium nitride reactive spray

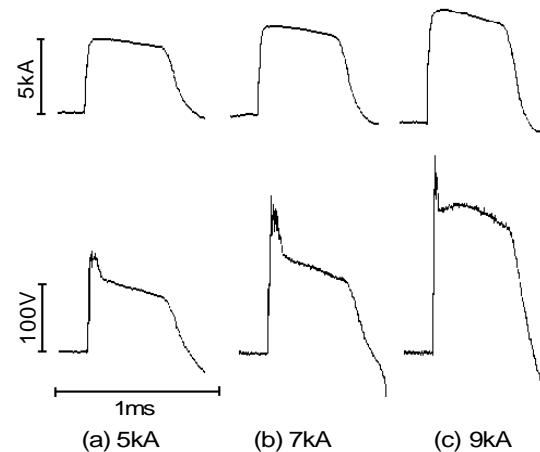
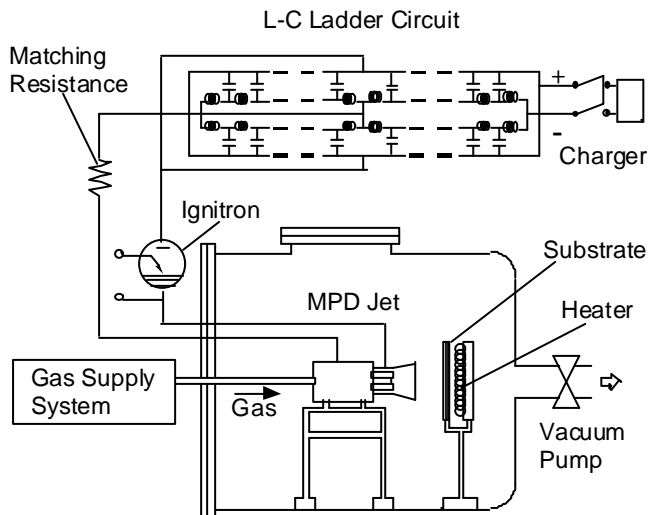


Fig.5 Experimental system with the MPD arcjet generator and the substrate stand installed in a vacuum tank. Fig.6 Typical waveforms of discharge current and voltage of the MPD arcjet generator for Mullite spray coating with Ar at 4.6 g/s.

2. Experimental Apparatus

Figure 2 shows the cross sectional view of the coaxial MPD arcjet generator developed for ceramic spray coatings. The MPD arcjet generator is equipped with a cathode 6 mm in diameter, of which the side surface is covered with a cylindrical ceramic material. The cathode is made of thoriated tungsten. The anode nozzle made of copper is 58 mm in exit diameter with a 20 degree half-angle. Mullite and Calcia-stabilized Zirconia are used as the ceramic material. The composition of the Mullite cover is Al_2O_3 56 wt%, SiO_2 41 wt% and CaO 3 wt%, and that for Zirconia is ZrO_2 94 wt%, CaO 4 wt% and Al_2O_3 2 wt%. The end of the ceramic material is set up at the same axial position as that of the upstream end of the discharge chamber, and the cathode end covered with the ceramic material is placed 5 mm recessed from the ceramic cover end. The ceramic material is supplied by turning the screw at the end of the arcjet generator body. Hence, as shown in Fig.3, ceramic particles are supplied to the discharge and acceleration zone by ablation of the ceramic cover due to a high current arc. Argon is mainly used as the working gas.

Another type of MPD arcjet generators for titanium nitride spray coating, as shown in Fig.4, is developed. The cathode is made of titanium, and its diameter can be changed from 6 to 10 mm. Nitrogen is used as the working gas. A high current arc is expected to melt the Ti cathode surface, and then the ablated Ti particles react on nitrogen plasma.

Working gases are injected into the discharge chamber through a fast acting valve (FAV) from a high pressure reservoir. The rise time and width of the gas pulse, measured with a fast ionization gauge, are 0.5 and 6 ms, respectively. The mass flow rates are controlled by adjusting the reservoir pressure and the orifice diameter of the FAV.

Figure 5 shows the experimental system with the MPD arcjet generator. The main power-supplying pulse forming network (PFN) is capable of storing 62 kJ at 8 kV and delivers a single nonreversing maximum quasi-steady current of 27 kA with a pulse width of 0.58 msec. A high PFN charging voltage is applied between the electrodes exactly at 3.4 ms after the gas pulse is triggered; arc discharge then begins. The interval between discharges is about 20 s, i.e., at a repetitive frequency of 0.05 Hz. The MPD arcjet generator is installed on a stand in a vacuum tank 1 m in diameter \times 1.2 m in length. The tank pressure is kept $2\text{-}5 \times 10^{-1}$ Pa during periodical operations. Unprepared substrate plates 4.5 mm thick, made of stainless steel SS400 for Mullite or Zirconia coating and of silicon for titanium nitride coating, are placed 100 mm downstream from the arcjet generator exit. The substrate temperature is kept constant in the range of 100-500 °C by an electrical heater placed behind the substrate.

Discharge currents are measured with a Rogowski coil calibrated with a known shunt resistance. Voltage measurement is performed with a current probe (Iwatsu CP-502), which detects the small current through a known resistor (10 k Ω) between the electrodes. Figure 6 presents the typical discharge current and voltage waveforms. The discharge voltage gradually increases with the discharge current for the MPD arcjet generator, and high input powers above 1 MW are achieved.

Front velocities of ablated particles of the ceramic component for the Mullite ceramic cover just after the start of discharge are inferred using a streak camera. The line spectrum of 396.1 nm, emitted from ablated aluminum atoms, is used, and the profiles are measured at a location 10 mm from the arcjet generator exit on the central axis. It was confirmed that the Al line spectrum was not observed using an MPD arcjet generator without a ceramic cover. Thus, we can simply evaluate front velocities of Al atoms using the streak camera, but not by using the time-of-flight or laser Doppler method^{5,6}.

Triple probe measurements are made to evaluate electron temperatures and electron number densities of the MPD arc plasmas, and emission spectroscopic measurements are also conducted to identify excited ion and atom species in the plasmas^{10,11}.

3. Flowfield Calculation

Axisymmetric MPD generator flowfield is numerically calculated in order to understand nitrogen plasma acceleration processes for titanium nitride spray¹². In this analysis, we assume that (1) velocities of

electron, ion, neutral are equal, i.e., one-fluid model; (2) electron temperature equals heavy species temperature, i.e., one temperature model; (3) nonequilibrium ionization process and first ionization are considered; (4) molecular vibration and rotation are not considered; (5) the Hall effect and viscosity are neglected; (6) heat conduction is considered, and (7) vapor and melted particles of titanium are neglected; i.e., only nitrogen fluid is analyzed. Conservation equations of mass, momentum and energy in addition to the magnetic field equation are a group of modified Euler equations.

The Total Variation Diminishing (TVD)-MacCormack scheme with Roe-Yee-Davis's dissipation term is used. In addition, a point-implicit method is also included in order to stabilize numerical oscillation due to chemical reaction terms, which are sensitive to temperature. The induction equation of magnetic field is solved by the successive over relaxation method, and time-dependent term is removed because we want to get only a steady-state solution. A steady-state solution is obtained by solving both the Euler equations and the magnetic field equation alternatively with coupling them together.

4. Results and Discussion

4.1 Discharge voltage, ablation rate and discharge chamber condition after Mullite spraying

Mullite and Zirconia ceramic sprayings are performed using the MPD arcjet generator with Ar at a gas mass flow rate of 4.6 g/s. The weights of the ceramic covers are measured before and after 110-shot operations, and the change in the weights, i.e., ablation rates, are estimated. After spraying, the ablated ceramic covers and the electrodes are observed, and the features of the ablation arc are recorded.

In 110-shot operations, the discharge voltages for Ar with the Mullite ceramic cover are about 130 and 230 V at discharge currents of 5 and 9 kA, respectively, as shown in Fig.6, although they were 40-60 V with no ceramic cover^{5,6}. After 110 shots, the inner diameter of the ceramic cover increased to about 8 mm. The ablation rates of the Mullite ceramic cover were 4.1 and 8.1 mg/shot at 8 and 9 kA, respectively, and that of the Zirconia ceramic cover was 1.8 mg/shot at 9 kA. The difference in ablation ratio between the Mullite and Zirconia ceramic covers is expected to be due to their difference in melting temperature. On the inner surfaces of the ceramic covers many axial grooves had been formed due to current spokes. Since the entire discharge current flows in the narrow ceramic cover, the ablation of the ceramic material is expected to intensively occur. After 110 shots, both electrodes were negligibly eroded although in the x-ray diffraction pattern of the Mullite coating the signals of tungsten are observed as mentioned below.

4.2 Ablated aluminum atom velocity for Mullite spraying

The front velocity of ablated Al atoms of the ceramic component for Mullite ceramic coating, just after the start of discharge, is estimated. The front velocities with the Mullite ceramic cover for Ar and 1.37 g/s ranged from 3.0 to 4.7 km/s at discharge currents of 5-10 kA and for H₂ and 0.40 g/s from 4.0 to 5.4 km/s^{5,6}. The velocity increased with the discharge current, although they were much lower than average exhaust plasma velocities estimated from reaction forces^{5,6}. The front velocity with H₂ was higher for the lower molecular weight. It is noteworthy that the velocities of ablated Al atoms evaluated are much higher than velocities of 200-500 m/s for conventional plasma torches for ceramic spraying. This is expected because the ablated Al atoms are drastically accelerated in a cathode jet confined by the strong azimuthal magnetic field. This property is effective for the deposition of rigid films adhering strongly to substrate surfaces.

4.3 Coating characteristics for Mullite and Zirconia sprayings

Figures 7 and 8 show the cross-sectional photographs and the x-ray diffraction patterns of the Mullite and Zirconia coatings in the 110-shot operation for Ar and 4.6 g/s at 9 kA with a substrate temperature of 400 °C. Dense uniform films 30 and 10 μm in thickness for Mullite and Zirconia, respectively, are deposited. The structure for the Mullite coating is an amorphous one although that for the Zirconia coating is a crystal one. This is explained as follows. For Mullite, melting, evaporation and decomposition of the structure are enhanced although for Zirconia the raw structure remains. This is because the melting and evaporating temperatures for Mullite are much lower than those for Zirconia. As a result, all particles decomposed for Mullite cannot be crystallized because of intensive cooling on the substrate. Also, the signals of tungsten, emitted from the cathode eroded, are observed in the Mullite coating. However, in cases below a discharge current of 8 kA, the signals hardly appeared in the XRD pattern. Accordingly, low current operations are preferable for Mullite spraying, that is, for sprayings of low melting-temperature materials.

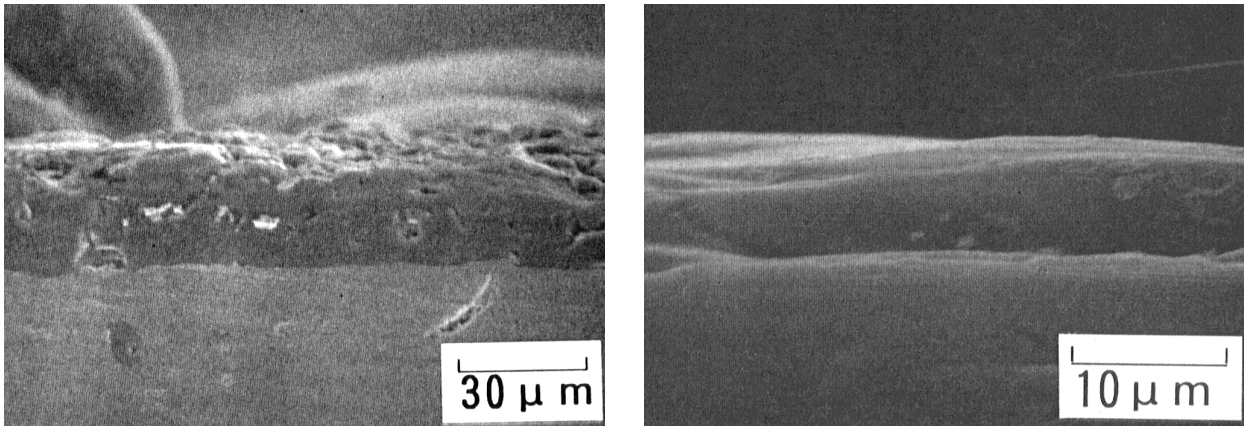
As shown in Fig.9, the Vickers hardness of the Mullite coating at 9 kA reaches about 1000 at the central position. A hard film with above 800 Vickers hardness is deposited within 20 mm in diameter from the

substrate center at 8 and 9 kA. The hardness for the Mullite coating decreases with decreasing discharge current at a constant radial position. Furthermore, the hardness with 400 was higher than that with 300^{8,9)}. From the XPS spectra of the Mullite coating and the raw ceramic material, it was found that the peak area ratio of Si/Al for the coating almost equaled that for the raw ceramic cover and that the valence numbers of Al and Si were unchanged.

4.4 Coating characteristics for titanium nitride reactive spraying

The MPD arcjet generator for titanium nitride reactive spraying is operated with 50 shots for N₂ and 2.5 g/s at discharge currents of 6-12 kA. The substrate temperature is kept 400 during the spraying. The weights of the titanium cathode are measured before and after 50 shots, and the change in the weights, i.e., ablation rates are estimated.

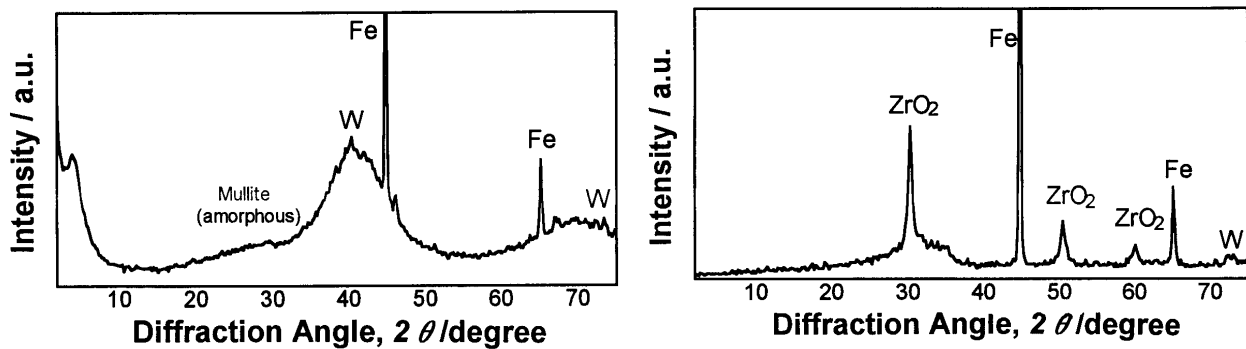
Figures 10, 11 and 12 show the cross-sectional photographs, the x-ray diffraction patterns and the



Vickers

(a) (b)

Fig.7 Photograph of cross sections for Mullite and Zirconia spray coatings after 110 shots with Ar, 4.6 g/s and 400 at 9 kA. (a) Mullite; (b) Zirconia.



(a) (b)

Fig.8 X-ray diffraction patterns for Mullite and Zirconia spray coatings after 110 shots with Ar, 4.6 g/s and 400 at 9 kA. (a) Mullite; (b) Zirconia.

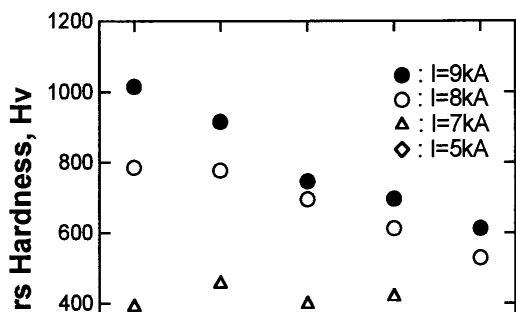
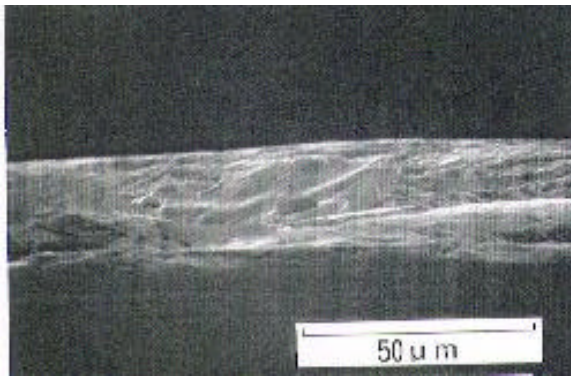
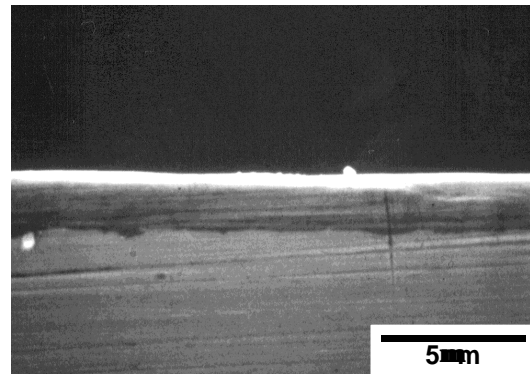


Fig.9 Radial profiles of Vickers hardness for Mullite spray coating after 110 shots at Ar, 4.6 g/s and 400 with varying discharge current. hardness of the coatings dependent on cathode diameter. Dense and uniform titanium nitride coatings are deposited onto the substrate. The thickness decreases from 40 μ m with the 6-mm-diam. cathode to 3 μ m with the 10-mm-diam. cathode. The

Vickers hardness, as shown in Fig.12, is highly sensitive to the cathode diameter and the discharge current. It increases with increasing cathode diameter at a constant discharge current. As a result, a maximum Vickers hardness of about 1000, is achieved at the substrate center with 10 mm. In the coating structure, as shown in Fig.11, a TiN, Ti₂N and Ti mixed layer is observed with the 6-mm-diam. cathode. However, the contents of Ti and Ti₂N decrease with increasing cathode diameter; that is, a TiN ratio comes to be dominant. With the 10-mm-diam. cathode, a TiN mono layer can be constructed. The XRD characteristics agree with the Vickers hardness. These results are explained as follows. Since the current density on the cathode increases with

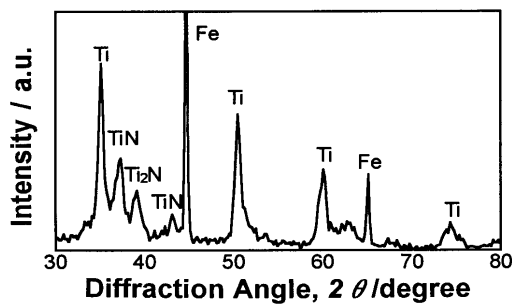


(a)



(b)

Fig.10 Photograph of cross sections for titanium nitride reactive spray coating after 50 shots for cathode diameters of 6 and 10 mm with N₂, 2.5 g/s and 400 at 10 kA. (a) 6 mm; (b) 10 mm.



(a)

(b)

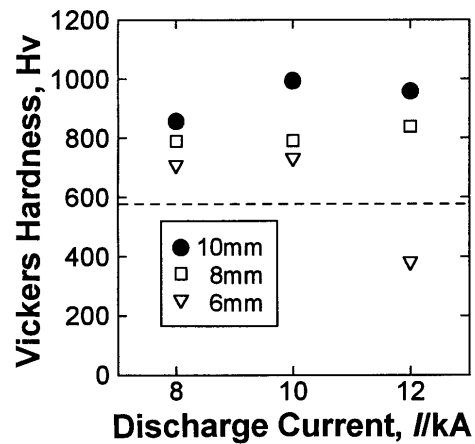
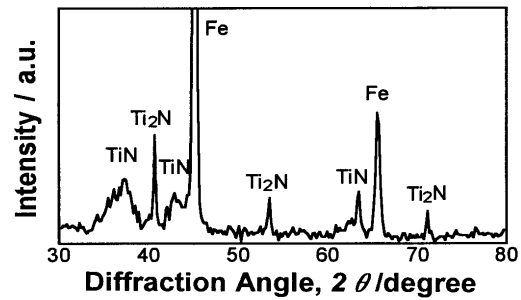
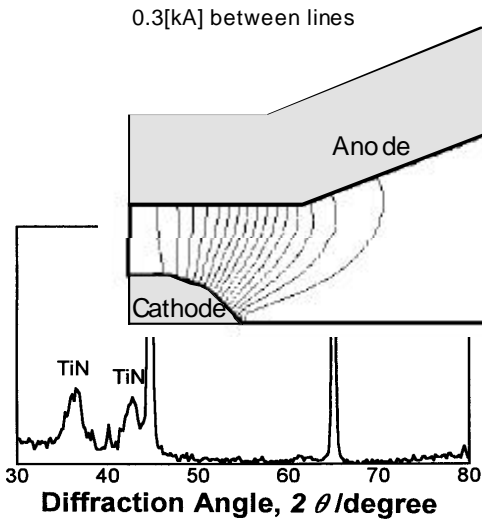


Fig12 Vickers hardness vs discharge current characteristics for titanium nitride reactive spray coating dependent on titanium cathode diameter after 50 shots with N_2 , 2.5 g/s and 400 at 10 kA.

increasing cathode diameter, an amount of titanium ablated by current concentration on the cathode decreases. The ablation rate of titanium was greatly

(c)

Fig.11 X-ray diffraction patterns for titanium nitride reactive spray coating dependent on titanium cathode diameter after 50 shots with N_2 , 2.5 g/s and 400 at 10 kA. a) 6 mm; b) 8 mm; c) 10 mm.



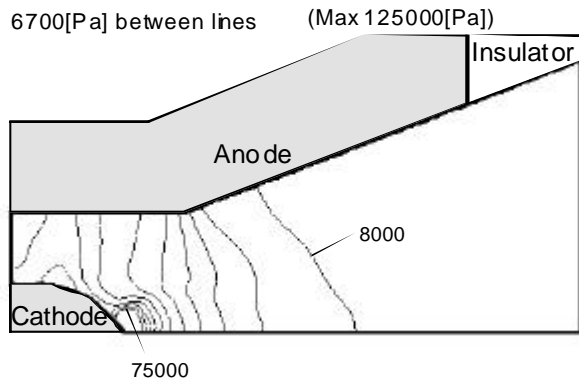
(a)

changed from 15.1 mg/shot with the 6-mm-diam. cathode to 0.34 mg/shot with the 10-mm-diam. cathode at 10 kA. In other words, when the cathode with the largest diameter of 10 mm is used, the TiN-richest coating is constructed by suppressing supply of excess of titanium from the cathode. Accordingly, the coating characteristics are sensitive to cathode diameter; that is, MPD flowfield characteristics dependent on cathode diameter

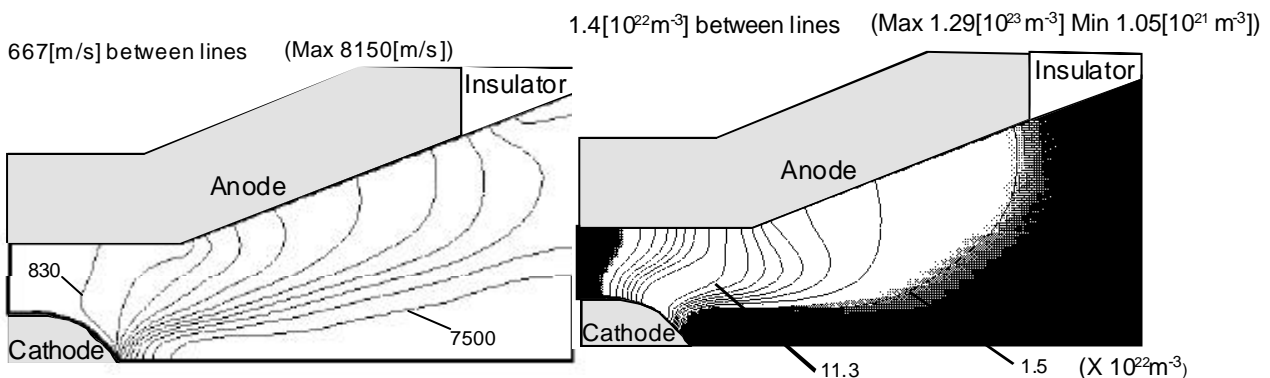
4.5 Plasma characteristics for titanium nitride reactive spraying

4.5.1 Inner plasma flowfield features

Figure 13 shows the calculation results of the distributions of discharge current, axial velocity, temperature, pressure, and number densities of nitrogen



(d)



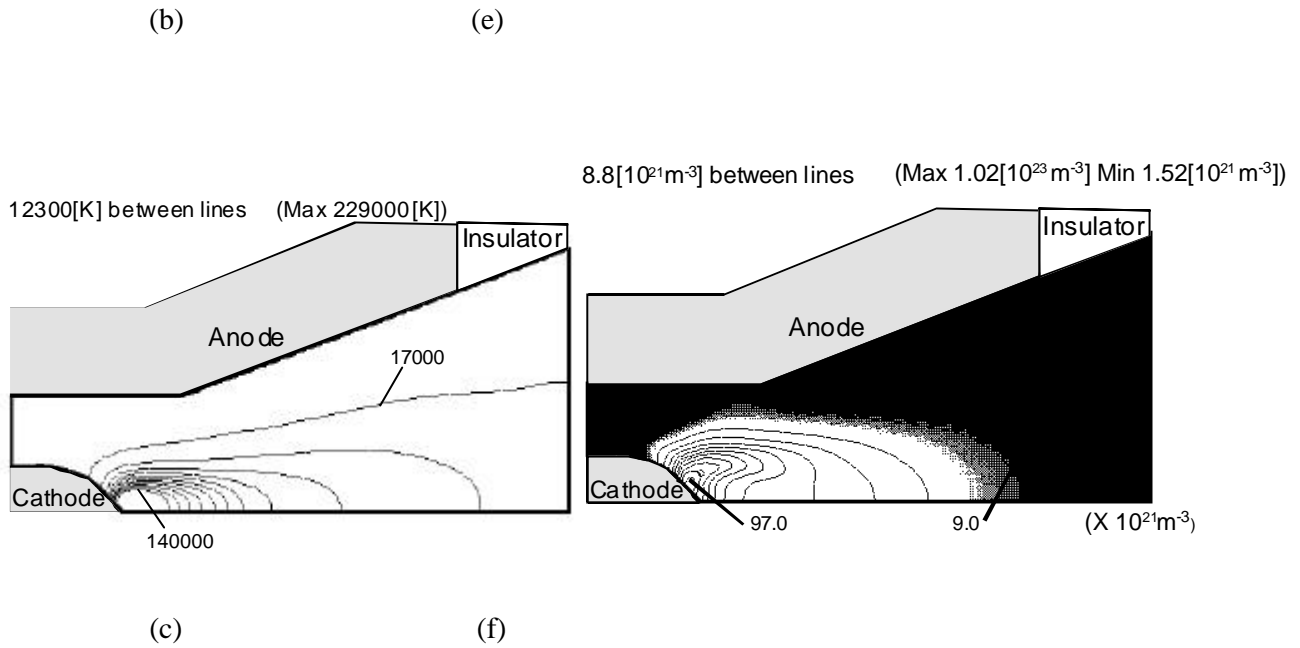
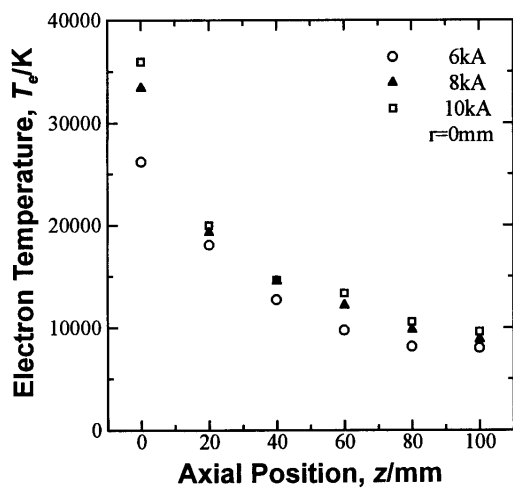
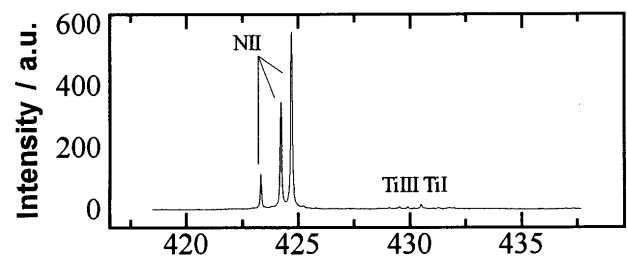
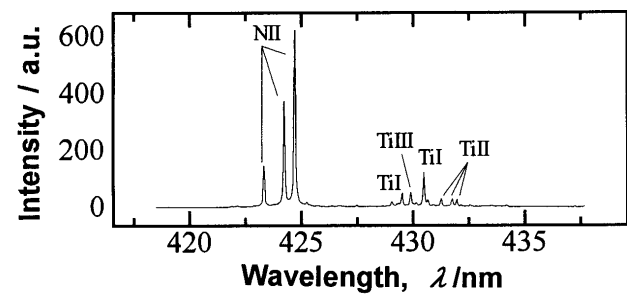
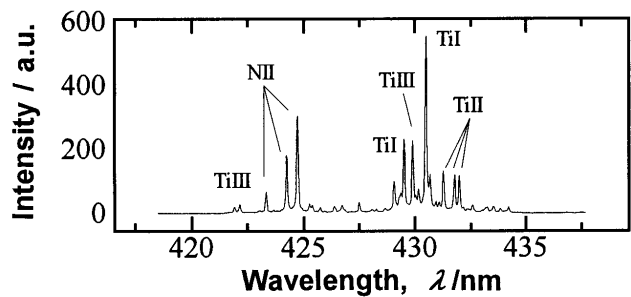
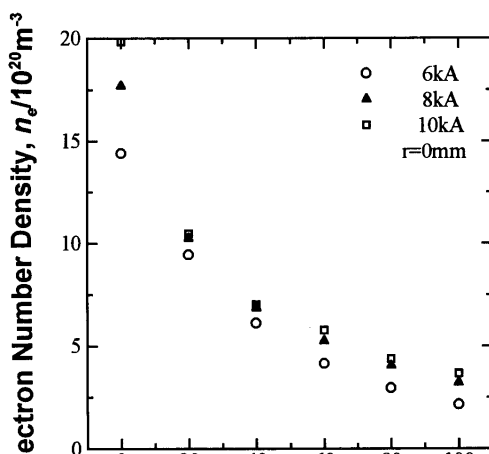


Fig.13 Calculation results of distributions of physical properties in the MPD arcjet generator with a cathode diameter of 10 mm for N₂ and 2.5 g/s at 6 kA. (a) Discharge current; (b) Axial velocity; (c) Temperature; (d) Pressure; (e) Number density of N; (f) Number density of N⁺.



(a)



(b) (c)

Fig.14 Axial variations of electron temperature and electron number density on the central axis in the downstream region of the cathode-ablation-type MPD arcjet generator for titanium nitride reactive spray coating with a cathode diameter of 10 mm at N_2 and 2.5 g/s. (a) Electron temperature; (b) Electron number density.

Fig.15 Spectra observed perpendicular to the central axis at 100 mm downstream from the exit of the cathode-ablation-type MPD arcjet generator for titanium nitride reactive spray coating with cathode diameters of 6, 8 and 10 mm at 10 kA at N_2 and 2.5 g/s. (a) 6 mm; (b) 8 mm; (c) 10 mm.

atom and nitrogen atomic ion in the MPD arcjet generator with a cathode diameter of 10 mm for N_2 and 2.5 g/s at 6 kA. The discharge current is concentrated at the cathode tip; melting and evaporation of the titanium cathode are expected to be enhanced by an intensive Joule heating at the cathode tip. As shown in Fig.13(b), plasma is drastically accelerated near the cathode tip by a strong Lorentz force, and it smoothly flows downstream from the cathode tip on the central axis; that is, it is named a cathode jet. The maximal velocity of 8150 m/s is achieved at the nozzle exit in the cathode jet. Both the temperature and the pressure reach the maximums of 2.29×10^5 K and 1.25×10^5 Pa, respectively, at the cathode tip. As shown in Fig.13(e), the number density of nitrogen atom is high in an interelectrode region upstream from the cathode tip and in a region from the side boundary of the cathode jet near the cathode to the anode surface, i.e., except in the cathode jet. In the regions, dissociation of nitrogen molecules is active because of Joule heating in the main current conduction region as shown in Fig.13(a). On the other hand, the number density of nitrogen ion, as shown in Fig.13(f), is very high near the cathode tip, i.e., in the cathode jet. As a result, a high-temperature, high-pressure and highly-ionized plasma is generated near the cathode tip. The number densities of N and N^+ are 8.7×10^{21} and $8.0 \times 10^{21} \text{ m}^{-3}$, respectively, at the nozzle exit on the central axis. Large amounts of chemically active particles of N and N^+ are expected to be exhausted with high velocities from the MPD generator.

4.5.2 Outer plasma flowfield features

Figure 14 shows the axial variations of electron temperature and electron number density on the central axis in the downstream region outside the MPD arcjet generator, in which the axial position of zero represents the MPD generator exit. The electron temperatures gradually decrease downstream from 25000-35000 K at the generator exit to 10000 K at an axial position of 100 mm. The electron temperature slightly increases with the discharge current at a constant axial position. The electron number densities also decrease downstream from $1.5\text{-}2.0 \times 10^{21} \text{ m}^{-3}$ to $2\text{-}3.5 \times 10^{21} \text{ m}^{-3}$. An increase in discharge current slightly raises the electron number density at a constant axial position. The electron number density measured at the MPD generator exit is lower than the calculated one as presented above. This is expected because of too simple model of calculation such as one-fluid, one-temperature and no wall losses etc. However, the calculation values are roughly acceptable within one order. Hence, both the electron temperature and the electron number density are kept high even at an enough downstream position of 100 mm, i.e., at the substrate position, compared with those for conventional low-pressure thermal sprayings.

Figure 15 shows the spectra observed perpendicular to the central axis at 100 mm downstream from the MPD generator exit with cathode diameters of 6, 8 and 10 mm at 10 kA. Since the intensive spectra of N^+ are observed regardless of cathode diameter, a chemically active plasma with a large amount of excited nitrogen ions is expected to flow even at 100 mm as predicted from the calculation results. Furthermore, since the spectra of Ti atom, Ti^+ and Ti^{2+} ions are observed, the excited titanium particles in addition to the excited nitrogen ions are expected to contribute to the titanium nitride reactive spray coatings.

The spectral intensities of titanium relatively decrease with increasing cathode diameter compared with those of N^+ . This agrees with the coating characteristics as mentioned above; that is, an amount of excited titanium particles with the 6-mm-diam. cathode are larger than that with the 10-mm-diam. cathode because an amount of titanium supplied by melting and evaporation with 6 mm is larger than that with 10 mm. Hence, taking account of these spectral characteristics, when the spectral intensities of N^+ are relatively high

and those of titanium are very low; that is, with a larger diameter cathode, high-quality titanium nitride films, i.e., TiN-rich films are expected to be created.

5. Conclusions

Two types of MPD arcjet generators were developed for applications of them to ceramic spray coatings. One was provided with a cathode covered with Mullite or Zirconia ceramics and the other with a titanium cathode. The former was operated with Ar for Mullite or Zirconia coating due to ablation of the cathode cover and the latter with N₂ for titanium nitride coating due to reactive process between ablated titanium particles and nitrogen plasma. The discharge voltage with the Mullite ceramic cover drastically increased compared with those with no ceramic cover, and both electrodes were negligibly eroded. The front velocity of ablated Al atoms for Mullite spraying was much higher than the velocities reported for conventional plasma torches. Uniform dense coatings were deposited with all experimental conditions. The structure for the Mullite coating was an amorphous one although that for the Zirconia coating was a crystal one. The Vickers hardness for the Mullite and titanium nitride coatings was above 1000. However, the thickness for the titanium nitride coating decreased with increasing cathode diameter although the hardness increased. In the coating structure, a TiN, Ti₂N and Ti mixed layer was observed with a small-diam. cathode. However, the contents of Ti and Ti₂N decreased with increasing cathode diameter; that is, a TiN ratio came to be dominant. With a large-diam. cathode, a TiN mono layer could be constructed. In titanium nitride reactive spraying, plasma diagnostic measurement and flowfield analysis were also made. A large amount of N and N⁺ was expected to be exhausted with a high velocity from the MPD generator. Both the electron temperature and the electron number density were kept high at a substrate position compared with those for conventional low-pressure thermal sprayings. A chemically active plasma with excited particles of N⁺, Ti, Ti⁺ and Ti²⁺ were expected to contribute to better titanium nitride coatings. Consequently, all coating characteristics showed that the MPD arcjet generators had high potentials for ceramic spray coatings.

References

- 1) R.G. Jahn, Physics of Electric Propulsion, McGraw-Hill, New York, 1968, Chap.8.
- 2) Tahara, H., Kagaya, Y. and Yoshikawa, T., "Quasisteady Magnetoplasmadynamic Thruster with Applied Magnetic Fields for Near-Earth Missions," *J. Propulsion and Power*, Vol.5, 1989, pp.713-717.
- 3) Tahara, H., Kagaya, Y. and Yoshikawa, T., "Effects of Applied Magnetic Fields on Performance of a Quasisteady Magnetoplasmadynamic Arcjet," *J. Propulsion and Power*, Vol.11, 1995, pp.337-342.
- 4) Tahara, H., Kagaya, Y. and Yoshikawa, T., "Performance and Acceleration Process of Quasisteady Magnetoplasmadynamic Arcjets with Applied Magnetic Fields," *J. Propulsion and Power*, Vol.13, 1997, pp.651-658.
- 5) Tahara, H., Abe, T., Tsubaki, T., Kagaya, Y., Tsubakishita, Y., Yoshikawa, T., Kuwata, M. and Ueda, Y., "Applications of Quasi-Steady Magneto-Plasma-Dynamic Arcjets to Ceramic Coatings," *Jpn. J. Appl. Phys.*, Vol.32, 1993, pp.5122-5128.
- 6) Tahara, H., Kagaya, Y. and Yoshikawa, T., "Development of a Magnetoplasmadynamic Arc Jet Generator for Ceramic Coatings," Proc. Int. Thermal Spraying Conf., Kobe, 1995, pp.295-300.
- 7) Tahara, H., Matsuda, M., Shibata, T., Andoh, Y., Yasui, T., Kagaya, Y. and Yoshikawa, T., "Research and Development of a Magnetoplasmadynamic Arc Jet Generator for Ceramic Spray Coatings," Proc. Int. Symp. Designing, Processing and Properties of Advanced Engineering Materials, Toyohashi, 1997, pp.529-534.
- 8) Tahara, H., Shibata, T., Andoh, Y., Yasui, T., Kagaya, Y. and Yoshikawa, T., "Electromagnetic Acceleration Plasma Spraying for Ceramic Coatings," Proc. United Thermal Spray Conf, Dusseldorf, 1999, pp.715-719.
- 9) Tahara, H., Shibata, T., Yasui, T., Kagaya, Y. and Yoshikawa, T., "Electromagnetic Acceleration Plasma Spraying," Proc. 14th Int. Symp. Plasma Chemistry, Praha, Vol.4, 1999, pp.1977-1981.
- 10) Shibata, T., Tahara, H., Yasui, T. and Yoshikawa, T., "Plasma Flow Characteristics of Electromagnetic Acceleration Plasma Jet Generators for Titanium-Nitride Reactive Spray Coatings," Proc. 15th Int. Symp. Plasma Chemistry, Orleans, Vol.6, 2001, pp.2219-2224.
- 11) Tahara, H., Kagaya, Y. and Yoshikawa, T., "Exhaust Plume Characteristics of Quasi-Steady MPD Thrusters," 27th Int. Electric Propulsion Conf., Pasadena, IEPC-01-133, 2001.
- 12) Tahara, H., Mitsuo, K., Kagaya, Y. and Yoshikawa, T., "Magnetoplasmadynamic Channel Flow Research," 35th Joint Propulsion Conf., Los Angeles, AIAA-99-2431, 1999.